Backstepping Control of Dual Stator Induction Generator used in Wind Energy Conversion System

BENAKCHA Meryem *, BENALIA Leila *, TOURQUI Djamel Eddine **,

BENAKCHA Abdelhamid***

* Electrical engineering Laboratory (LGE), M'sila University, BP 166, Algeria

** Energy Engineering and Computer Engineering Laboratory (L2GEG), Tiaret University, BP 78, Algeria

*** Electrical engineering Laboratory of Biskra (LGEB), Biskra University, BP 45, Algeria

(benakcha.meryem@gmail.com, leila_bena@yahoo.fr, tourqui.djamel@gmail.com, ab.benakcha@gmail.com)

‡ Corresponding Author; BENAKCHA Meryem, BP 166, Algeria, Tel: +213 664492465,

benakcha.meryem@gmail.com

Abstract- This paper presents the wind energy conversion system with a variable speed of wind turbine connected to the grid based on the dual stator induction generator (DSIG) which is controlled by backstepping technique approach. DSIG is increasingly used because of its advantages as better reliability and supply division. DSIG consists of two fixed three-phase stator windings which necessitates having in parallel two converters with a displaced angle of 30° between the two sources and being controlled at the same time. The use of the classical PI regulators has shown some limitations in their synthesis. Due to this down side, the aim of this work is to apply the backstepping technique for replacing the PI controller into a field oriented control (FOC) structure. The backstepping technique is a systematic and recursive method of synthesis of nonlinear control laws from the Lyapunov functions which ensure step by step the stabilization of each synthesis step. With this algorithm, the feedback control law is constructed to control the power produced from the wind energy. The effectiveness of the proposed control is demonstrated through an illustrative simulation.

Keywords- Variable Speed, Wind Turbine, Maximum Power Point Tracking (MPPT), Dual Stator Induction Generator, Field Oriented Control, Backstepping Control.

1. Introduction

In the development of any country, the energy plays a vital role. For centuries, wind energy has been used to provide mechanical work [1]. The best known example is the windmill used by the miller to process wheat into flour. Subsequently, for several decades, wind energy was used to generate electrical energy in remote locations and thus not connected to an electrical grid. Installations without energy storage imply that the energy requirement and the presence of wind energy must be simultaneous. The control of the storage of energy in batteries allows to store this energy and the multiplication of domestic electrical appliances and lets to considerable planetary needs in electrical energy [2]. Since

the 1990s, the improvement of wind turbine technology permits to build wind turbines of more than 5 MW and the development of wind turbines of 10 MW is under way [3]. These wind turbines are used today to produce alternating current for power grids, as well as a nuclear reactor, a hydroelectric dam or a coal-fired power plant. However, the powers generated and the impacts on the environment are not the same [4, 5]. Wind energy is the cleanest energy that does not directly produce carbon dioxide, sulfur dioxide, mercury or fine particles. It is an abundant source of energy entirely free [6]. The wind conversion system is composed of minimum elements able to optimize the transfer of the wind energy. Ideally, only one turbine, one transmission shaft, one rotating electrical generator and unidirectional or

bidirectional electronic converters are required [7].The mechanical characteristics of the wind turbine, the conversion efficiency of the mechanical energy into electrical energy are very important [8]. Many devices exist and, for the most part, they use synchronous or asynchronous machines. The control strategies of these machines and their possible interfaces to the network must make it possible to capture as much energy as possible over a range of wind speed variation in order to improve the profitability of wind installations [9]. The studied system here consists of an aero generator three-bladed, with horizontal axis, connected to the network by the dual stator induction generator (DSIG). In term of wind energy and grid integration, it is very interesting to produce a quality output power. Therefore, the control of the generator is very important. Many techniques have been used to control the DSIG such as a sliding mode control (SMC) associated to the field oriented control [10], Genetic Algorithm Optimized PI and Fuzzy Logic Speed Vector Control [11], model reference adaptive system based reactive power controller [12], nonlinear method based on the theory of fuzzy logic controlled torque [13], control of the DSIG using the instantaneous power theory and a control flux orientation at low speeds [14].

This type of machines has some advantages compared to other types of induction machines, such as power segmentation, minimizing torque ripples, reducing rotor harmonic currents and the use of the latter in wind projects of which powers are of a few MW [10, 15]. A high performance control device requires in general a good response in regulation and must be not very sensitive to the variations of operating conditions and system parameters [16]. There are a nonlinear control techniques that present simplicity of implementation interest and a facility of the regulators gains synthesis. The application of these techniques requires also the knowledge of the system parameters [17]. Backstepping control is part of these new control methods. It is a recursive technique used in increasingly complex systems. It was developed by Kanellakopoulos and al. (1991) which were inspired by the works of Feurer and Morse (1978) on the one hand and Tsinias (1989) and Kokotovic & Sussman (1989) on the other [18,19,20]. The basic idea of backstepping control is to make looped systems equivalent to cascaded first order subsystems, stable in the sense of Lyapunov, which gives it robust qualities and an asymptotic global stability [21]. The paper aims to present the backstepping control law for the DSIG used in the wind energy conversion system connected to the grid. This law is established step by step while ensuring the stability of the loop machine closed. The mathematical model of the entire system should be studied and detailed. The obtained results using Matlab/Simulink software will be examined and interpreted.

2. Wind Turbine and gearbox modeling

The power available by derivation of the kinetic energy of the air mass passing through the surface S swept by the turbine is [22]:

$$P_w = 0.5\rho SV^3 \tag{1}$$

In this expression, V represents the wind speed assumed to be constant over the entire surface S.
The power coefficient can be defined by:

$$C_p = \frac{P_t}{P_w} \tag{2}$$

So, this power coefficient C_p is the aerodynamic efficiency of a wind turbine and its evolution is specific to each turbine and wind speed. It depends on the blade pitch angle β and the speed ratio λ which is expressed by:

$$\lambda = \frac{R\Omega_t}{V} \tag{3}$$

where R is the blade radius.

In this work, we use for the power coefficient the following expression [3]:

$$C_p = \left[0.73\left(\frac{151}{\lambda'}\right) - 0.002 - 13.2\right]\exp\left(\frac{-18.4}{\lambda'}\right) \tag{4}$$

With

$$\lambda' = \left[1/(\lambda + 0.08\beta) - 0.035/(\beta^3 + 1)\right]^{-1}$$

The transmitted power P_t, captured by the wind turbine, is given by [23,24]:

$$P_t = C_p(\lambda, \beta)\rho SV^3 \tag{5}$$

The torque of the turbine is the ratio of the transmitted power to the shaft speed Ω_t. It is given by:

$$T_t = \frac{P_t}{\Omega_t} \tag{6}$$

The optimum speed of the current turbines is in the vicinity of a few tens of revolutions per minute. This requires the introduction of a gearbox between the turbine and the electrical machine whose gear ratio G is chosen in order to set the generator shaft speed within a desired speed range. Neglecting the transmission losses, the torque T_g and shaft speed of the wind turbine Ω_t, referred to the generator side of the gearbox, are given by:

$$T_g = \frac{T_t}{G} \quad , \Omega_t = \frac{\Omega_{mec}}{G} \tag{7}$$

The mechanical equation can be expressed as:

$$Jp\Omega_{mec} = T_g - T_{em} - f\Omega_{mec} \tag{8}$$

For the value $\beta=0$, the graph of $C_p(\lambda)$, given in Fig.1, is plotted using expression (4).The conversion device extracts a power less than the theoretically recoverable power due to non-zero speed of air masses upstream of the turbine. This presents a theoretical limit called the Betz limit which corresponds to a C_{pmax} [3, 9].
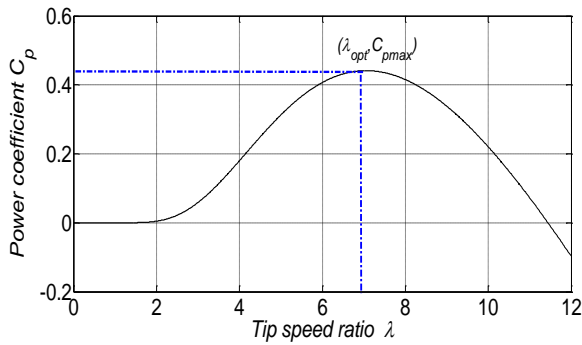
Fig. 1. The graph of C_p in function of λ.

The maximum power point tracking (MPPT) algorithm permits to maximize the electric power extracted from the wind energy [8, 23]. The tip speed ratio should be kept around its optimal value λ_{opt}. The reference speed Ω^*_{mec} can be written as:

$$\Omega^*_{mec} = \left(\frac{R\lambda_{opt}}{V}\right).G \tag{9}$$

The block diagram of the turbine model with the control of the speed is represented in Fig.2.
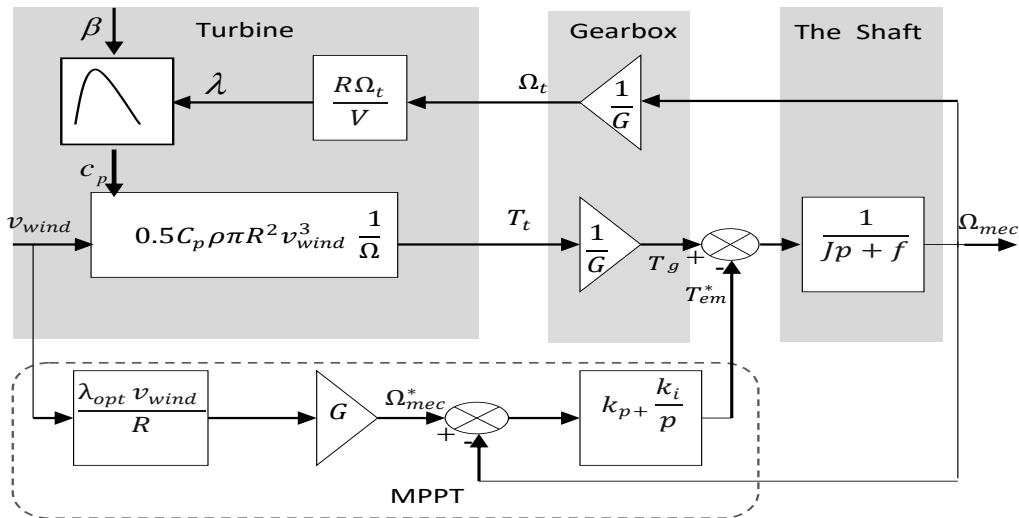
Fig. 2. Block diagram of the turbine model with variable speed control.

3. Modeling of the DSIG

The dual stator induction generator (DSIG) consists of a mobile rotor winding and two fixed three-phase stator windings displaced with an electrical angle $\alpha = 30°$. The windings axes of each star are displaced with an electrical angle $2\pi/3$ and fed by a balanced voltages system, creating a slipping magnetic field in the air-gap. The rotor is a squirrel cage consisting of conducting bars short-circuited by a conductive ring at each end. Fig.3 shows schematically the windings of the DSIG. The quantities relating to the two stars (1 and 2) will be denoted by s1 and s2 respectively. The mathematical model of the DSIG is derived from the PARK theory in order to simplify the differential equations as shown in Fig.3 [10, 13, 15].
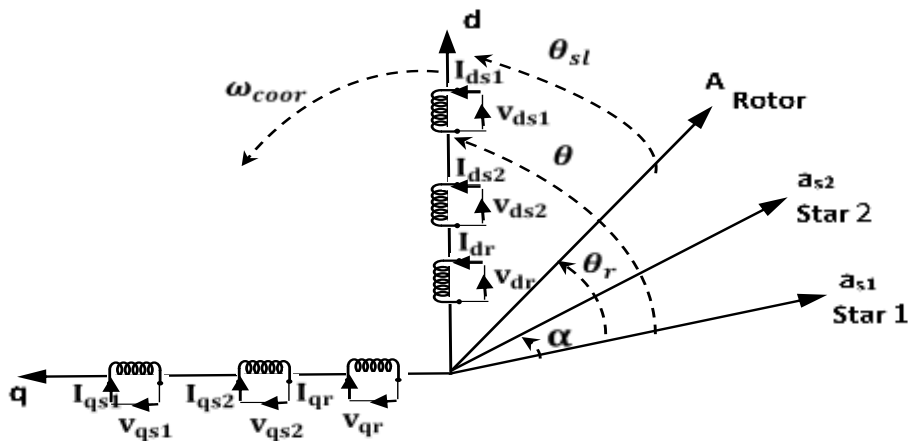
Fig. 3. Schematic of DSIG in (dq) frame.

The simulation of the DSIG is carried out using the state representation [21]:

$$[\dot{I}] = [L]^{-1}\{[B][U] - \omega_{gl}[C][I] - [D][I]\} \qquad (10)$$

Where:

$\omega_{gl} = \omega_s - \omega_r,\ \omega_r = p * \Omega_{mec}$

$[U] = [v_{ds1}\ v_{qs1}\ v_{ds2}\ v_{qs2}\ v_{dr}\ v_{qr}]^t$

$[I] = [\iota_{ds1}\ \iota_{qs1}\ \iota_{ds2}\ \iota_{qs2}\ \iota_{dr}\ \iota_{qr}]^t$

$$[\dot{I}] = \frac{d}{dt}[I]$$

$$[B] = \text{diag}\,[1\ 1\ 1\ 1\ 0\ 0]$$

$$[C] = \begin{bmatrix} 0 & 0 & 0 & 0 & 0 & 0 \\ 0 & 0 & 0 & 0 & 0 & 0 \\ 0 & 0 & 0 & 0 & 0 & 0 \\ 0 & 0 & 0 & 0 & 0 & 0 \\ 0 & -L_m & 0 & -L_m & 0 & -(L_r+L_m) \\ L_m & 0 & L_m & 0 & L_r+L_m & 0 \end{bmatrix}$$

$$[D] = \begin{bmatrix} R_{s1} & -\omega_s(L_{s1}+L_m) & 0 & -\omega_s L_m & 0 & -\omega_s L_m \\ \omega_s(L_{s1}+L_m) & R_{s1} & \omega_s L_m & 0 & \omega_s L_m & 0 \\ 0 & -\omega_s L_m & R_{s2} & -\omega_s(L_{s2}+L_m) & 0 & -\omega_s L_m \\ \omega_s L_m & 0 & \omega_s(L_{s2}+L_m) & R_{s2} & \omega_s L_m & 0 \\ 0 & 0 & 0 & 0 & R_r & 0 \\ 0 & 0 & 0 & 0 & 0 & R_r \end{bmatrix}$$

$$[L] = \begin{bmatrix} (L_{s1}+L_m) & 0 & L_m & 0 & L_m & 0 \\ 0 & (L_{s1}+L_m) & 0 & L_m & 0 & L_m \\ L_m & 0 & (L_{s2}+L_m) & 0 & L_m & 0 \\ 0 & L_m & 0 & (L_{s2}+L_m) & 0 & L_m \\ L_m & 0 & L_m & 0 & (L_r+L_m) & 0 \\ 0 & L_m & 0 & L_m & 0 & (L_r+L_m) \end{bmatrix}$$

The electromagnetic torque is expressed by:

$$T_{em} = P\frac{L_m}{(L_m+L_r)}\left[(\iota_{qs1} + \iota_{qs2})\varphi_{dr} - (\iota_{ds1} + \iota_{ds2})\varphi_{qr}\right] \quad (11)$$

The active and reactive powers are described by:

$$\begin{cases} P_s = v_{ds1}\iota_{ds1} + v_{qs1}\iota_{qs1} + v_{ds2}\iota_{ds2} + v_{qs2}\iota_{qs2} \\ Q_s = v_{qs1}\iota_{ds1} - v_{ds1}\iota_{qs1} + v_{qs2}\iota_{ds2} - v_{ds2}\iota_{qs2} \end{cases} \qquad (12)$$

3.1. Field oriented control of DSIG

The control laws of the FOC are derived from the DSIG equations by the Park transformation related to the rotating field (d, q) and the rotor flux orientation [10,25].The model of the DSIG expressed in (d, q) frame is given by:

$$\begin{cases} \dot{i_{ds1}} = \frac{1}{L_1}\{v_{ds1} - r_1\iota_{qs1} - \omega_s^*(L_1\iota_{ds1} + \varphi_{dr}^*)\} \\ \dot{\iota_{qs1}} = \frac{1}{L_1}\{v_{qs1} - r_1\iota_{ds1} + \omega_s^*(L_1\iota_{qs1} + \tau_r\varphi_{dr}^*\omega_{sl}^*)\} \\ \dot{i_{ds2}} = \frac{1}{L_2}\{v_{ds2} - r_2\iota_{qs2} - \omega_s^*(L_2\iota_{ds2} + \varphi_{dr}^*)\} \\ \dot{\iota_{qs2}} = \frac{1}{L_2}\{v_{qs2} - r_2\iota_{ds2} + \omega_s^*(L_2\iota_{qs2} + \tau_r\varphi_{dr}^*\omega_{sl}^*)\} \\ \dot{\varphi_{dr}}^* = -\alpha\varphi_{dr} + \alpha L_m(\iota_{sd1} + \iota_{sd2}) \\ \dot{\Omega} = \frac{1}{J}\left[\mu\varphi_{dr}^*(\iota_{sq1} + \iota_{sq2}) - T_r - f_r\Omega\right] \end{cases} \qquad (13)$$

3.2. Backstepping control of DSIG

The objective of the backstepping type control that we are going to synthesize is to allow the control of the output variables (flux, speed). To impose a trajectory on these outputs, we have chosen, as intermediate variables, the stator currents that must follow their reference values defined by the command. Finally, we compute the necessary voltage commands (stator voltages) by respecting at each step the stability of the associated Lyapunov function [20]. The synthesis of the regulators is therefore divided into two parts. However, the system must be in the pure parametric form, to apply the Backstepping control, the system must be in strict feedback form [26, 27].

A. Step 1:

In order to design a control law of the backstepping type allowing the tracking in speed and in flux for the machine, we define the errors of tracking in speed and flux:

$$\begin{cases} e_1 = \Omega^* - \Omega_{mec} \\ e_2 = \varphi_{dr}^* - \varphi_{dr} \end{cases} \qquad (14)$$

The derivatives of (14) are:

$$\begin{cases} \dot{e}_1 = \dot{\Omega}^* - \dot{\Omega}_{mec} \\ \dot{e}_2 = \dot{\varphi_{dr}}^* - \dot{\varphi}_{dr} \end{cases} \qquad (15)$$

The first Lyapunov function is chosen as:

$$V_1 = \frac{1}{2}(e_1^2 + e_2^2) \qquad (16)$$

Its derivative is:

$$\dot{V}_1 = e_1\dot{e}_1 + e_2\dot{e}_2$$

$$= e_1[\dot{\Omega}^* - \frac{1}{J}[\mu(\iota_{qs1} + \iota_{qs2})\varphi_{dr}^* - T_r - f_r\Omega] +$$
$$e_2[\dot{\varphi_{dr}}^* - [-\alpha\varphi_{dr} + \alpha L_m(\iota_{ds1} + \iota_{ds2})]] \qquad (17)$$

The basic idea of the Backstepping method consists in calculating a control law in order to guarantee that the derivative of the Lyapunov function is always negative ($\dot{V}_1 < 0$), by choosing the references of the current components that represent the stabilizing functions as follows:

$$\begin{cases} \iota_{qs1}^* + \iota_{qs2}^* = \frac{J}{\mu\varphi_{dr}^*}[K_1e_1 + \dot{\Omega}^* + \frac{T_r}{J} + \frac{f_r\Omega}{J}] \\ \iota_{ds1}^* + \iota_{ds2}^* = \frac{1}{\alpha L_m}[K_2e_2 + \dot{\varphi_{dr}}^* + \alpha\varphi_{dr}] \end{cases} \qquad (18)$$

where K_1, K_2 are positive constants.

We suppose that the two stars have the same values of the reference currents:

$$\iota_{ds1}^* = \iota_{ds2}^* , \quad \iota_{qs1}^* = \iota_{qs2}^*.$$

B. Step2:

For this step, our objective is to calculate the control voltages. Other errors concerning the components of the stator currents and their references are first defined:

$$\begin{cases} e_3 = \iota_{qs1}^* - \iota_{qs1} \\ e_4 = \iota_{ds1}^* - \iota_{ds1} \\ e_5 = \iota_{qs2}^* - \iota_{qs2} \\ e_6 = \iota_{ds2}^* - \iota_{ds2} \end{cases} \qquad (19)$$

With this definition and taking into account the system (13) the derivatives of (19) are written:

$$\begin{cases} \dot{e}_3 = \dot{\iota_{qs1}^*} - \dot{\iota_{qs1}} = \dot{\iota_{qs1}^*} - \frac{1}{L_1}\{v_{qs1} + \sigma_1\} \\ \dot{e}_4 = \dot{\iota_{sd1}^*} - \dot{\iota_{ds1}} = \dot{\iota_{ds1}^*} - \frac{1}{L_1}\{v_{ds1} + \sigma_2\} \\ \dot{e}_5 = \dot{\iota_{qs2}^*} - \dot{\iota_{qs2}} = \dot{\iota_{qs2}^*} - \frac{1}{L_2}\{v_{qs2} + \sigma_3\} \\ \dot{e}_6 = \dot{\iota_{ds2}^*} - \dot{\iota_{ds2}} = \dot{\iota_{ds2}^*} - \frac{1}{L_2}\{v_{ds2} + \sigma_4\} \end{cases} \qquad (20)$$

Where:

$$\begin{cases} \sigma_1 = \frac{1}{L_1}\{-r_1\iota_{qs1} - \omega_s^*(L_1\iota_{ds1} + \varphi_{dr}^*)\} \\ \sigma_2 = \frac{1}{L_1}\{-r_1\iota_{ds1} + \omega_s^*(L_1\iota_{qs1} + \tau_r\varphi_{dr}^*\omega_{sl}^*)\} \\ \sigma_3 = \frac{1}{L_2}\{-r_2\iota_{qs2} - \omega_s^*(L_2\iota_{ds2} + \varphi_{dr}^*)\} \\ \sigma_4 = \frac{1}{L_2}\{-r_2\iota_{ds2} + \omega_s^*(L_2\iota_{qs2} + \tau_r\varphi_{dr}^*\omega_{sl}^*)\} \end{cases}$$

The final Lyapunov function is given by:

$$V_2 = \frac{1}{2}(e_1^2 + e_2^2 + e_3^2 + e_4^2 + e_5^2 + e_6^2) \qquad (21)$$

Its derivative in function of time is:

$$\dot{V}_2 = e_1\dot{e}_1 + e_2\dot{e}_2 + e_3\dot{e}_3 + e_4\dot{e}_4 + e_5\dot{e}_5 + e_6\dot{e}_6$$

$$= -K_1e_1^2 - K_2e_2^2 - K_3e_3^2 - K_4e_4^2 - K_5e_5^2 - K_6e_6^2$$
$$+e_3\left(K_3e_3 - \sigma_1 + \dot{\iota_{qs1}^*} - \frac{1}{L}v_{qs1}\right)$$
$$+e_4\left(K_4e_4 - \sigma_2 + \dot{\iota_{ds1}^*} - \frac{1}{L}v_{ds1}\right)$$
$$+e_5\left(K_5e_5 - \sigma_3 + \dot{\iota_{qs2}^*} - \frac{1}{L}v_{qs2}\right)$$
$$+e_6\left(K_6e_6 - \sigma_4 + \dot{\iota_{ds2}^*} - \frac{1}{L}v_{ds2}\right)$$

Where K_3, K_4, K_5, K_6 are positive constants.
The control voltages are selected like:

$$\begin{cases} v_{qs1}^* = L_1[K_3e_3 - \sigma_1 + \dot{\iota_{qs1}^*}] \\ v_{ds1}^* = L_1[K_4e_4 - \sigma_2 + \dot{\iota_{ds1}^*}] \\ v_{qs2}^* = L_2[K_5e_5 - \sigma_3 + \dot{\iota_{qs2}^*}] \\ v_{ds2}^* = L_2[K_6e_6 - \sigma_4 + \dot{\iota_{ds2}^*}] \end{cases} \qquad (22)$$

The stability of the control is obtained if and only if a good choice of gains K_3, K_4, K_5, K_6 is made.
Fig.4. shows the block diagram of the proposed control design.
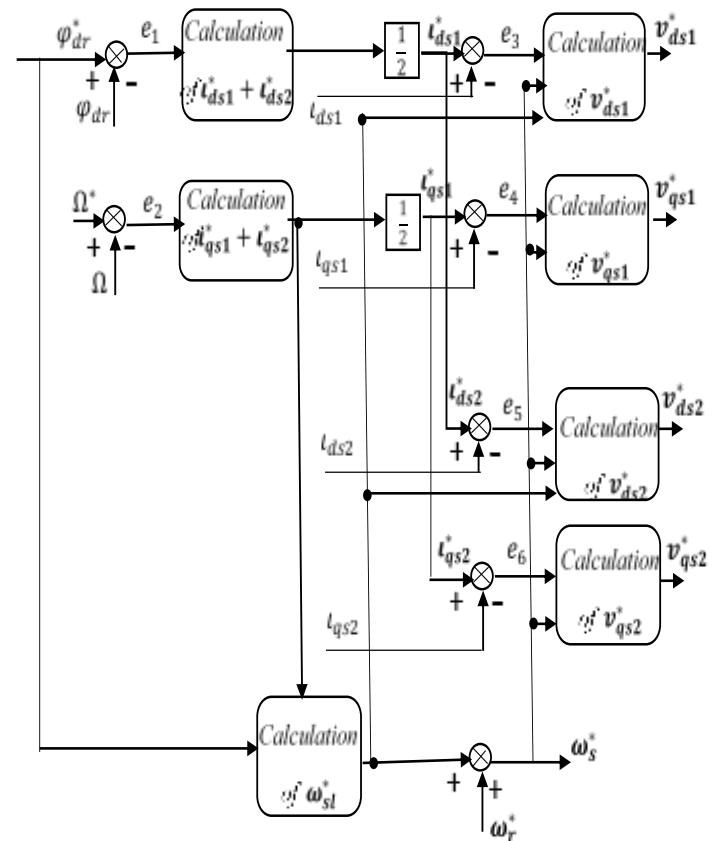
Fig. 4. Block diagram of the proposed backstepping control for DSIG

4. Grid Side Power Control

The inverter 3 in Fig.6 is connected between the DC bus and the electrical network through RL filter. This inverter has two functions: to keep the DC bus voltage constant, irrespective of the amplitude and direction of the power flow and to maintain a unit power factor at the point of connection with the electrical network [28].

The mathematical modeling of the studied DC link system is as follows [29]:

$$\frac{dU_{dc}}{dt} = \frac{1}{C}(\iota_{dc} - \iota_m)$$ (23)

Where:

$$\iota_{dc} = \iota_{d1} + \iota_{d2},$$

Network reference currents expressions can be represented by:

$$\begin{cases} \iota_{dg}^* = \frac{P_g^* v_{dg} + Q_g^* v_{qg}}{v_{dg}^2 + v_{qg}^2} \\ \iota_{qg}^* = \frac{P_g^* v_{qg} - Q_g^* v_{dg}}{v_{dg}^2 + v_{qg}^2}, \end{cases}$$ (24)

The network currents are expressed as:

$$\begin{cases} \iota_{dg} = \frac{1}{(R_t + L_t s)}(v_{d\_inv} - v_{dg} - L_t \omega_s \iota_{qg}) \\ \iota_{qg} = \frac{1}{(R_t + L_t s)}(v_{q\_inv} - v_{qg} + L_t \omega_s \iota_{dg}) \end{cases}$$ (25)

The grid active and reactive powers are described by:

$$\begin{cases} P_s = v_{dg}\iota_{dg} + v_{qg}\iota_{qg} \\ Q_s = v_{qg}\iota_{dg} - v_{dg}\iota_{qg} \end{cases}$$ (26)

The block diagram of the control loops for the currents axis (d, q) is described in Fig.5. The correctors used are of the PI type. This block diagram includes the terms of decoupling and compensation in order to be able to independently control the currents circulating in the RL filter and the active and reactive powers exchanged between the CCR and the network.
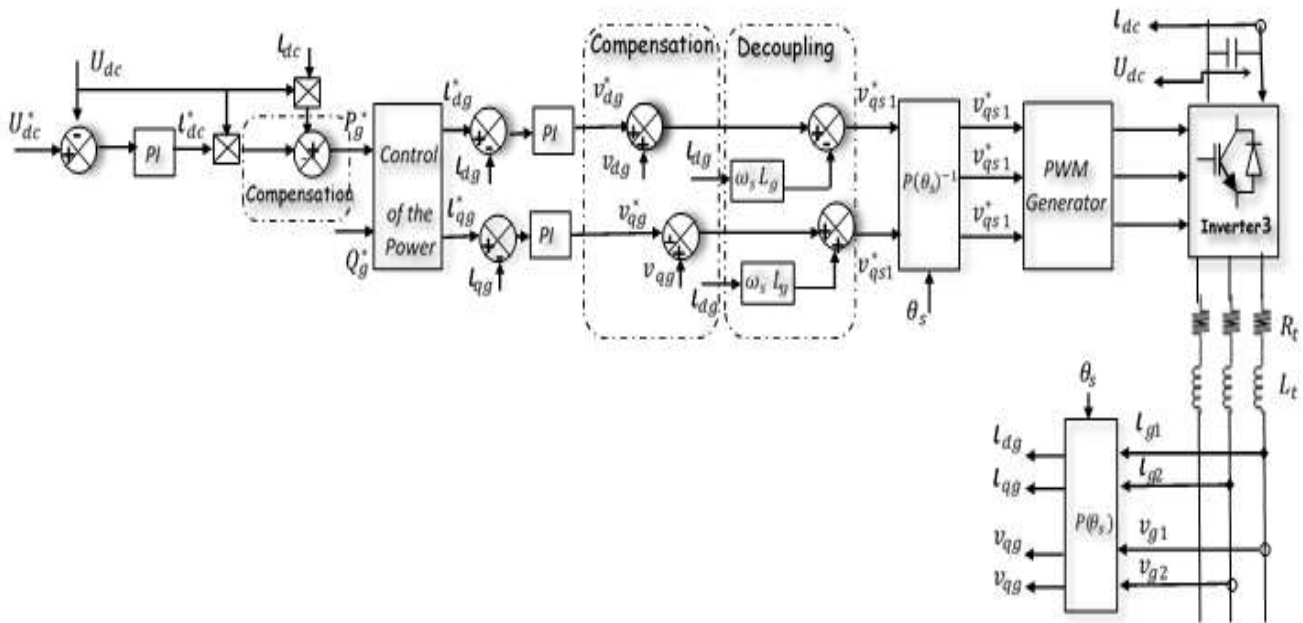
Fig. 5. Block diagram of the grid side power control.

The synoptic scheme of the studied system is shown in Fig.6.
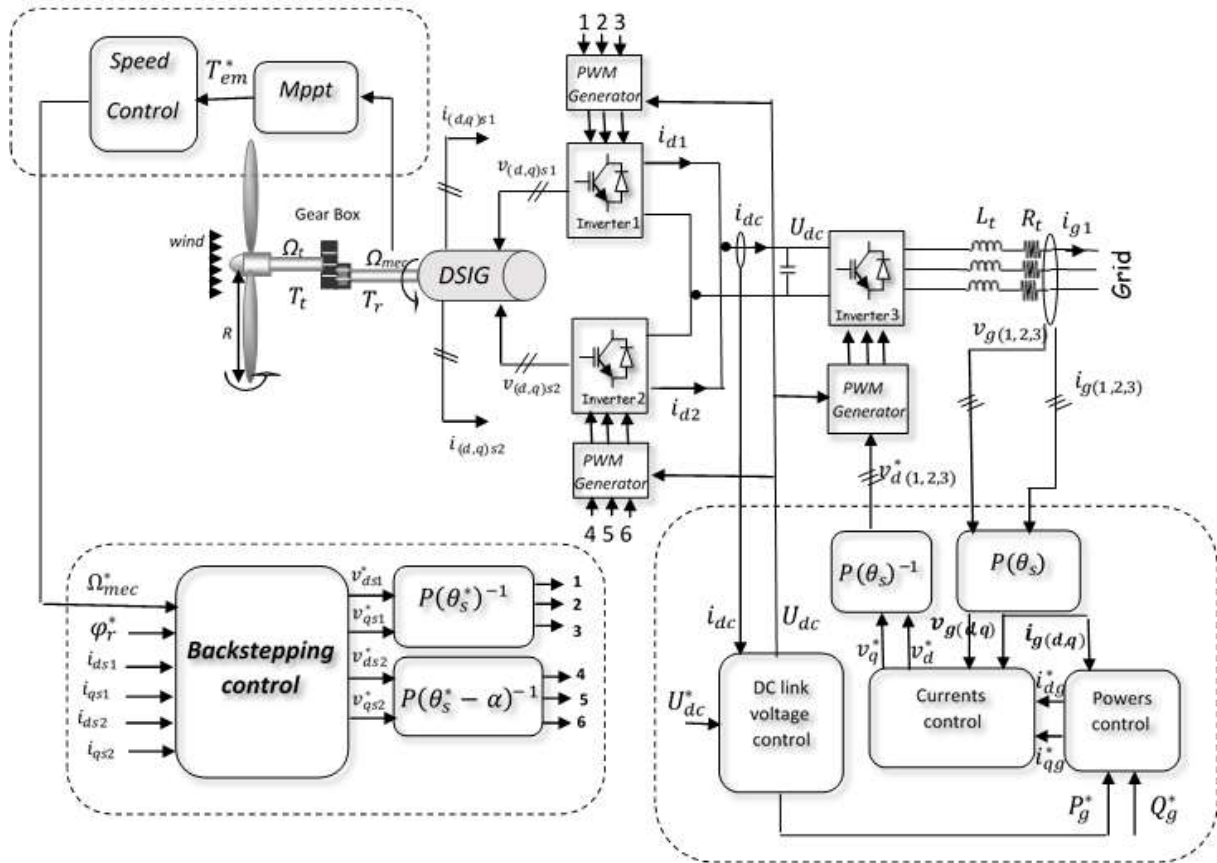
Fig. 6. Bloc diagram of the global wind conversion system based on DSIG

5. Simulation Results and Discussion

The simulation results of the control system, already presented, are implemented using Matab/Simulink software for the wind speed profile and power coefficient max depicted in Fig.7 and Fig.8 respectively. The overall control scheme is summarized in FIG. 6. All of its blocks are first programmed separately using the expressions detailed in the text. Only the basic elements of the Simulink library are used with fixed step size of sampling frequency 10^{+4} Hz. The DSIG used in this work is of 1.5 MW, whose nominal parameters are indicated in appendix.

It is clear from Fig.9 that the rotation speed follows perfectly its reference, which varies depending on the imposed wind profile. We can see from Fig.10 that the speed error, given by e1, converges to zero rapidly. The waveform of the electromagnetic torque generator follows its reference resulting from the MPPT algorithm as shown in Fig.11. The evolution of DSIG stator currents in the first phase of each star between (10.99 and 11.06 s) is shown in Fig.12. These currents are sinusoidal and displaced with $\alpha = 30°$.

The direct rotor flux of the DSIG and its reference is illustrated in Fig.13.We can find in Fig.14, that the rotor flux error, given by e2, converges to zero. The voltage and current grid and their zoom are given in Fig.15.a and b respectively. It is clear that the current has sinusoidal form

and opposite phase with respect to the voltage, meaning that power flows from the aero generator to the grid. The DC link voltage in Fig.16 is constant and follows its set level 1130 V. Fig.17 in turn, gives the spectrum THD (total harmonic distortion) of the grid current I_{g1}. It is defined as the ratio of total effective value of harmonics (their quadratic sum) to the rms value of the fundamental component. We will analyze a sequence of time. As we see, the harmonics appearing in the grid current are minimized. It can be seen from Fig.18 and 19 that the active and reactive grid powers follow in an acceptable way in accordance to their references at all simulation time. In order to get a unit power-factor in network side, the reactive power reference Q_g^* is fixed at zero value.
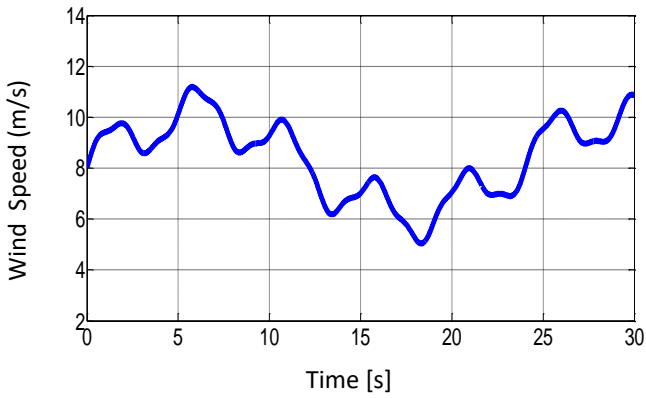
Fig. 7. Profile of wind speed.
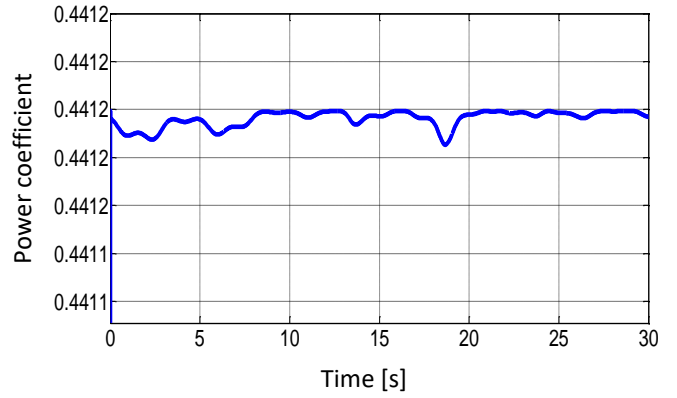
Fig. 8. Power Coefficient C_p.
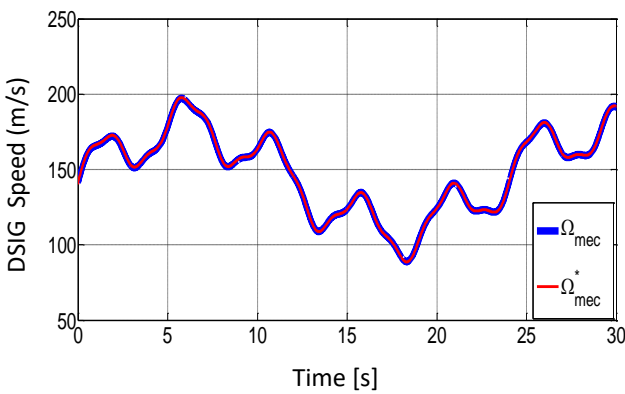
Fig. 9. DSIG speed and its reference.
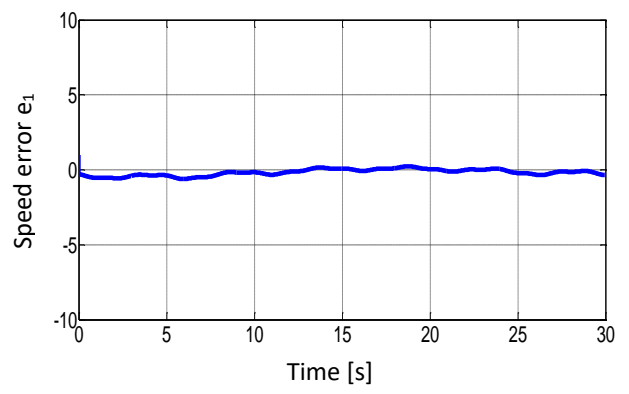
Fig. 10. DSIG speed error.
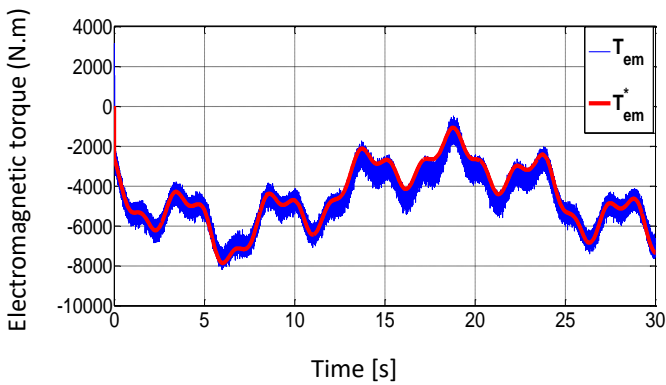
Fig. 11. DSIG Torque and its reference.
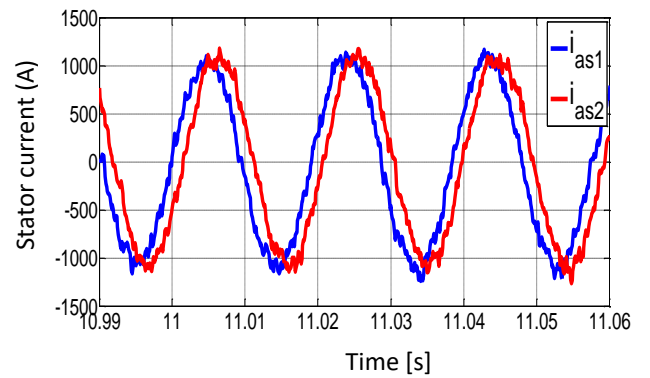
Fig. 12. Zoom of Stator currents.
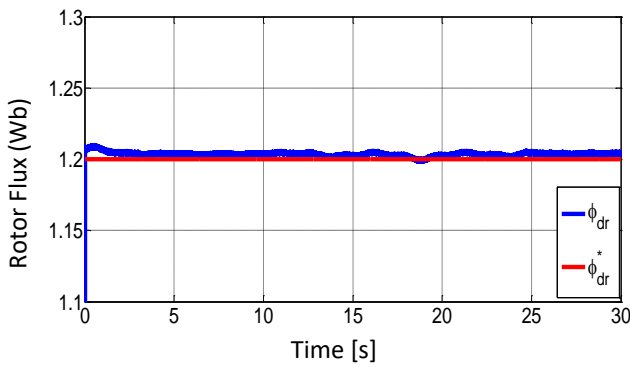
Fig. 13. Direct rotor flux.
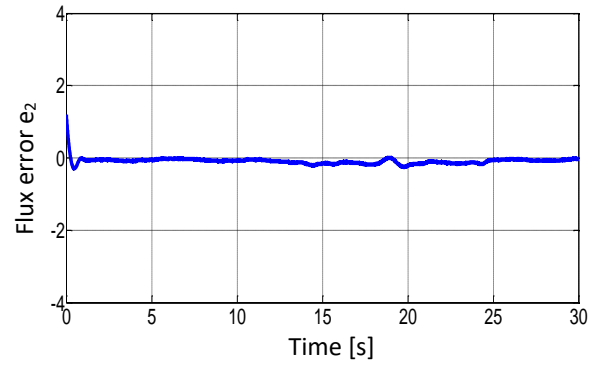
Fig. 14. Direct rotor flux error.
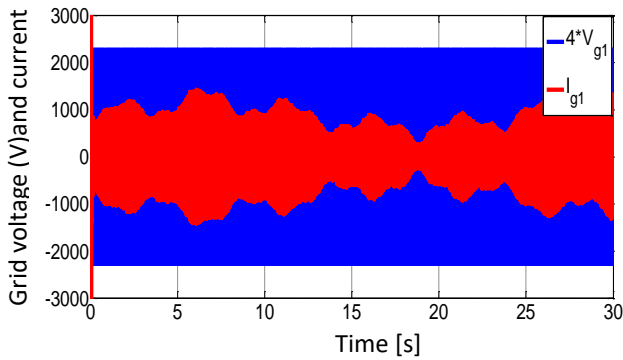
Fig. 15.a. Grid voltage and current.
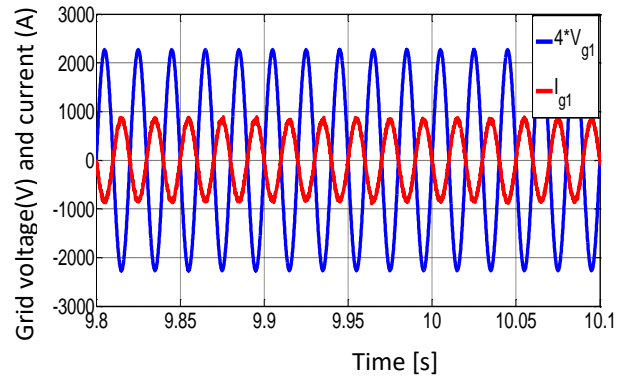
Fig. 15.b. Zoom of the grid voltage and current.
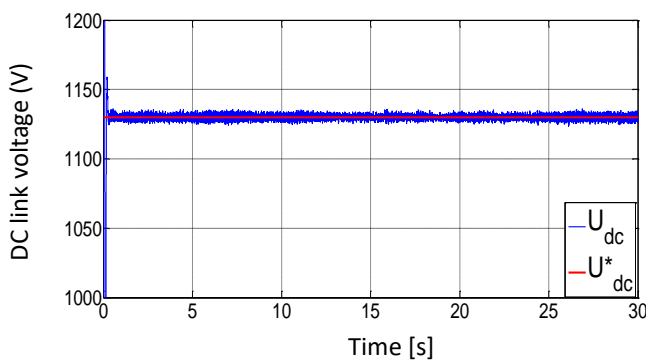
Fig.16. DC link voltage.
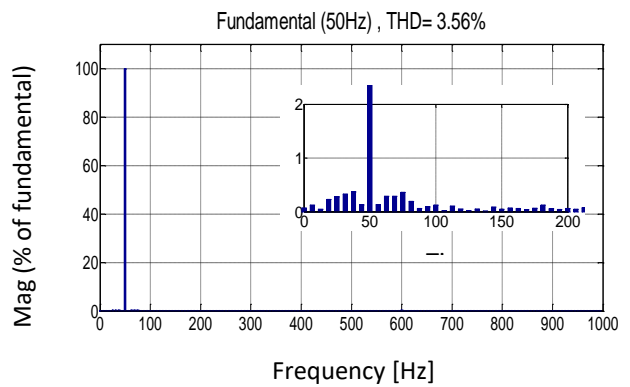
F**ig.17.**THD spectrum analysis of
the grid current Ig1.
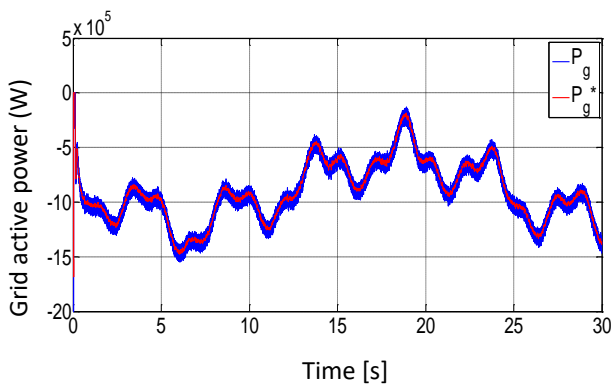
Fig. 18. Grid active power and its reference.
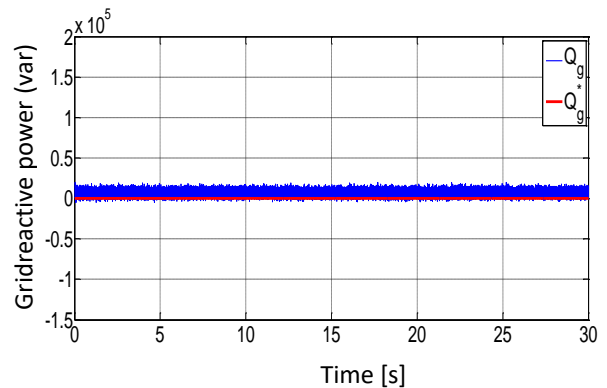
Fig. 19. Grid reactive power and its reference.

A. *Performance of the system to a voltage dip of 20%*

A voltage dip is a sudden drop in the supply voltage at one point of an electrical power network. The voltage dips are characterized by their amplitude and duration. They are the most common cause of power quality problems. Voltage dips are caused by events leading to high currents, which generate a voltage drop over at least significant through the impedances of the network elements. In this section, we will test the performance of our system with respect to a symmetrical fault voltage varying in amplitude

and duration corresponding to a voltage dip of 20% to be held at t = 10s and disappear at t = 15s. As the DSIG operates in steady state, the voltage and current grid of the default network during 5s are shown in Fig. 20 a and 20 b.

The variation of the active and reactive power generated in function of time is shown in Fig.21 and 22 respectively. After a short transitional phase the active and reactive grid powers follow in an acceptable way their references, even with default.
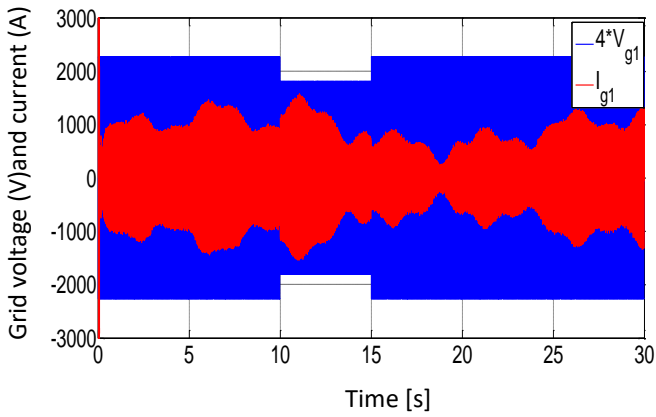
Fig. 20.a. Grid voltage and current.
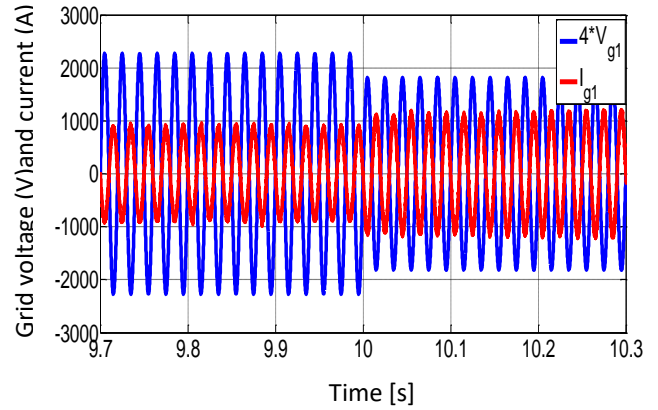
Fig. 20.b. Zoom of the grid voltage and current
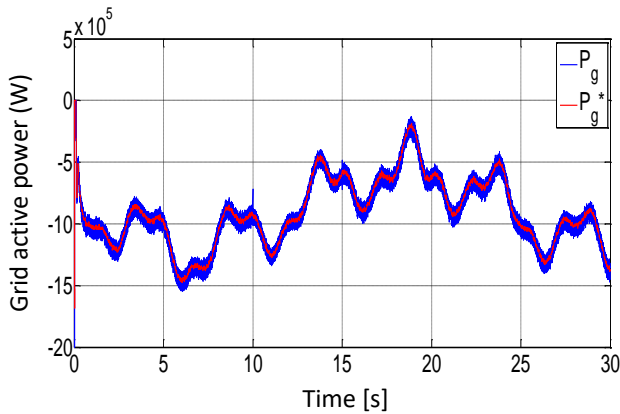
Fig. 21. Grid active power and its reference.
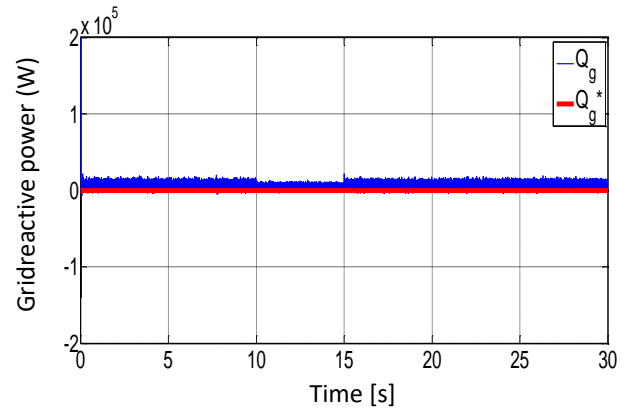
Fig. 22. Grid reactive power and its reference.

Table. 1. Appendix parameters

Turbine				
R (m)	Number of blades	G	C_{pmax}	λ_{opt}
36	3	90	0.44	7.05

DSIG								
P_n(MW)	U(V)	F(Hz)	Pair poles	R_{s1}, R_{s2} (Ω)	L_{s1}, L_{s2} (mH)	L_m (H)	J (kg.m^2)	Friction coefficient f (Nm.s/rd)
1.5	400	50	2	0.008	0.134	0.0045	10	2.5

Backstepping parameters					
K_1	K_2	K_3	K_4	K_5	K_6
50	10	20000	20000	20000	20000

Grid parameters		
L_t (H)	R_t (Ω)	C(F)
0.001	0.01	0.072

6. Conclusion

This work has been conducted to present the modeling and the simulation of a wind turbine with variable speed in order to maximize energy extraction from the wind.The turbine is connected to the grid through a DSIG which increasingly used in high power systems, in spit of its several advantages. It has some complexity in implementation of its control strategy. For this drawback, a nonlinear backstepping technique is proposed in order to get a flexible control which

ensure the stability of the system. A simulation results allow us to show the proposed algorithm capabilities, in terms of regulation, tracking and disturbance rejection, and demonstrating the robustness of this technique. For example, it can advantageously replace conventional PI control. From a conceptual point of view, we can notice that the backstepping control is simpler and easier to implement and has very interesting global stability properties

A control vector is achieved to control independently the grid active and reactive powers. Good results were obtained

with respect to the adjustment of the parameters. To improve the effectiveness and the performance of the control system we complete our study by treating the influence of a voltage dip on the wind conversion system. The control strategy of the entire system brings a satisfactory results and robust performance.

Nomenclature

L_m	Magnetizing inductance
R_r	Rotor resistance
L_r	Rotor inductance
J	Inertia moment
f	Viscous coefficient
ω_{gl}	Sliding speed
ω_s	Synchronous reference frame Speed
ω_r	Rotor electrical angular speed
Ω_{mec}	Mechanical speed of the DSIG
$v_{ds1}\ v_{qs1}\ v_{ds2}\ v_{qs2}$	d-q stator voltages
$v_{dr}v_{qr}$	d-q rotor voltages
$\iota_{ds1}\ \iota_{qs1}\ \iota_{ds2}\ \iota_{qs2}$	d-q stator currents
$\iota_{dr}\ \iota_{qr}$	d-q rotor currents
L_t	Filter inductance
R_t	Filter resistance
C	capacitance of the DC link voltage

References

[1] R. Aubrée, F. Auger, M. Macé, L. Loron, "Design of an efficient small wind-energy conversion system with an adaptive sensorless MPPT strategy", Renewable Energy, vol. 86, pp. 280-291, 2016.

[2] A. Gaillard, "Système éolien basé sur une MADA: contribution à l'étude de la qualité de l'énergie électrique et de la continuité de service", Doctorate Thesis, Henri Poincaré university, Nancy-I. 2010.

[3] A. Tamaarat, A. Benakcha, "Performance of PI controller for control of active and reactive power in DFIG operating in a grid-connected variable speed wind energy conversion system", Front. Energy, vol. 8, no.3, pp. 371–378, 2014.

[4] E. Aydin, A. Polat, L.T. Ergene,"Vector control of DFIG in wind power applications", IEEE International Conference on Renewable Energy Research and Applications (ICRERA), doi :10.1109 /ICRERA. 2016.7884383, pp. 478-483, 23 Nov 2016.

[5] P. Daoutidis, M. Zachar, S. Jogwar, "Sustainability and process control: A survey and perspective", Journal of Process Control, vol. 44, pp.184–206, 2016.

[6] M. Doumi, I. Colak , A. G. Aissaoui, M. Abid, A. Tahour, "Robust MRAC for a wind turbine based on a doubly-fed induction generator", IEEE 6th International Conference on Renewable Energy Research and

Applications (ICRERA), doi:10.1109/ ICRERA. 2017.8191236, pp. 1160-1165. 8 Nov 2017.

[7] K. Bedoud, M. Ali-rachedi, T. Bahi, R Lakel, "Adaptive Fuzzy Gain Scheduling of PI Controller for control of the Wind Energy Conversion Systems", Energy Procedia, vol. 74, pp. 211 – 225, 2015.

[8] G. Brando, A. Del Pizzo, P. Di Noia Luigi, S. Meo, " Second order variable structure control for wind turbine PMSG-based and generator-side converter system", IEEE International Conference on Renewable Energy Research and Applications (ICRERA), doi:10.1109/ ICRERA.2017.8191169, pp.797-801, 8. Nov 2017.

[9] K. Kajiwara, S. Kuboyama, T. Higuchi, J.W. Kolar, F. Kurokawa, "A new digital current control AC-DC converter for wind turbine", IEEE International Conference on Renewable Energy Research and Applications (ICRERA) doi:10.1109/ ICRERA. 2016.7884429, pp.726-729, 23 Nov 2016.

[10] H. Amimeur, D. Aouzellag, R. Abdessemed, K. Ghedamsi, "Sliding mode control of a dual-stator inductionFor wind energy conversion systems", Electrical Power and Energy Systems, vol. 42, 60–70, 2012.

[11] F. Ameur, K. Kouzi, "Genetic Algorithm Optimized PI and Fuzzy Logic speed Vector Control of Dual Stator Induction Generator in Wind Energy Conversion System", Proceedings of the third International Conference on Systems, Algiers, 29-31 October, 2013.

[12] S. Basak, C. Chakraborty, A. K. Sinha, "Dual Stator Induction Generator with Controllable Reactive Power Capability", 23rd International Symposium on Industrial Electronics (ISIE),IEEE. 2014.

[13] S. Chekkal, N. Aouzellag Lahaçani, D. Aouzellag, K. Ghedamsi, "Fuzzy logic control strategy of wind generator based on the dual-stator induction generator", Electrical Power and Energy Systems, vol. 59, pp. 166–175, 2014.

[14] F. Bu,Y. Hu ,W. Huang, S. Zhuang, K. Shi, "Wide-Speed-Range-Operation Dual Stator-Winding Induction Generator DC Generating System for Wind Power Applications", IEEE Transactions on Power Electronics, vol.30, no.2, February 2015.

[15] S. Lekhchine, T. Bahi, Y. Soufi, "Indirect rotor field oriented control based on fuzzy logic controlled double star induction machine", Electrical Power and Energy Systems, vol. 57, pp. 206–211. 2014.

[16] S. Elmetennani, T.M. Laleg-Kirati, M. D. Tadjine, "New MPPT algorithm for PV applications based on hybrid dynamical approach", Journal of Process Control, vol. 48, pp. 14–24, 2016.

[17] D. Pan, F. Wang, "Modeling and Simulation of Fuzzy Control System for Dual Stator Winding Induction Generator", Proceeding of International Conference on Electrical Machines and Systems, Seoul, Korea, 8-11 Oct, 2007.

[18] S. Mensou, A. Essadki, T. Nasser, B. Bououlid Idrissi, "An Efficient Nonlinear Backstepping Controller Approach of a Wind Power Generation System Based on a DFIG", International Journal of renewable Energy Research, Vol.7, No.4, 2017.

[19] A. Elmansouri, J. El mhamdi, A. Boualouch, "Control by Back Stepping of the DFIG Used in the Wind", International Journal of Emerging Technology and Advanced Engineering, vol. 5, pp. 472-478, 2015.

[20] A. Herizi, R. Balla, S.A. Ahmani, "Backstepping Control of Induction Motors", El Wahat pour les Recherches et les Etudes, vol. 8, pp. 132– 145, 2015.

[21] B. Bossoufi, M. Karim, A. Lagrioui, M. Taoussi, A. Derouich, "Observer backstepping control of DFIG-Generators for wind turbines variable-speed: FPGA-based implementation", Renewable Energy, vol. 81, pp. 903-917, .2015.

[22] Z. H. Kamali, Z. Salameh, A. Ashfaq, "Modeling of Wind Energy Conversion System using PSCAD/EMTDC", International Journal of renewable Energy Research, vol.7, no.1, 2017.

[23] S. Kahla, Y. Soufi, M. Sedraoui, M. Bechouat, "Maximum Power Point Tracking of Wind Energy Conversion System Using Multi-objective Grey Wolf Optimization of Fuzzy-Sliding Mode Controller", International Journal of renewable Energy Research, vol.7, no.2, 2017.

[24] M. Quraan, Q. Farhat , M. Bornat , "A new control scheme of back-to-back converter for wind energy technology", IEEE 6th International Conference on Renewable Energy Research and Applications (ICRERA), doi: 10.1109/ICRERA.2017.8191085, pp.354-358,8 Nov 2017.

[25] Z. Tir, O.P. Malik, A.M. Eltamaly, "Fuzzy logic based speed control of indirect field oriented controlled Double Star Induction Motors connected in parallel to a single six-phase inverter supply", Electric Power Systems Research, vol. 134, pp.126–133, 2016.

[26] N. Khemiri, A. Khedher, M.F. Mimouni, "Wind Energy Conversion System using DFIG Controlled by Backstepping and Sliding Mode Strategies", Int. J of Renewable Energy, vol. 2, no.3, 2012.

[27] Y. Hwang, K. Park, H, Yang. "Robust Adaptive Backstepping Control for Efficiency Optimization of Induction Motors with Uncertainties", In: IEEE International Symposium on Industrial Electronics, pp. 878-883, 2008.

[28] Y. Errami, M. Ouassaid, M. Maaroufi, "Optimal Power Control Strategy of Maximizing Wind Energy Tracking and Different Operating Conditions for Permanent Magnet Synchronous Generator Wind Farm", Energy Procedia, vol. 74, pp. 477 – 490, 2015.

[29] S. El Aimani, "Modélisation de différentes technologies d'éoliennes intégrées dans un réseau de moyenne tension", Doctorate Thesis, France : L2EP Central School of Lille, 2004.